Journal of Biomechanics 46 (2013) 1363–1368

Contents lists available at SciVerse ScienceDirect

Journal of Biomechanics

journal homepage: www.elsevier.com/locate/jbiomech
www.JBiomech.com

Defining feasible bounds on muscle activation in a redundant biomechanical task: practical implications of redundancy

M.Hongchul Sohn [a], J. Lucas McKay [b], Lena H. Ting [a,b,*]

[a] The George W. Woodruff School of Mechanical Engineering, Georgia Institute of Technology, GA, USA
[b] The Wallace H. Coulter Department of Biomedical Engineering, Georgia Institute of Technology and Emory University, GA, USA

ARTICLE INFO

Article history:
Accepted 20 January 2013

Keywords:
Motor control
Musculoskeletal model
Muscle redundancy
Cat hindlimb

ABSTRACT

Measured muscle activation patterns often vary significantly from musculoskeletal model predictions that use optimization to resolve redundancy. Although experimental muscle activity exhibits both inter- and intra-subject variability we lack adequate tools to quantify the biomechanical latitude that the nervous system has when selecting muscle activation patterns. Here, we identified feasible ranges of individual muscle activity during force production in a musculoskeletal model to quantify the degree to which biomechanical redundancy allows for variability in muscle activation patterns. In a detailed cat hindlimb model matched to the posture of three cats, we identified the lower and upper bounds on muscle activity in each of 31 muscles during static endpoint force production across different force directions and magnitudes. Feasible ranges of muscle activation were relatively unconstrained across force magnitudes such that only a few (0–13%) muscles were found to be truly "necessary" (e.g. exhibited non-zero lower bounds) at physiological force ranges. Most of the muscles were "optional", having zero lower bounds, and frequently had "maximal" upper bounds as well. Moreover, "optional" muscles were never selected by optimization methods that either minimized muscle stress, or that scaled the pattern required for maximum force generation. Therefore, biomechanical constraints were generally insufficient to restrict or specify muscle activation levels for producing a force in a given direction, and many muscle patterns exist that could deviate substantially from one another but still achieve the task. Our approach could be extended to identify the feasible limits of variability in muscle activation patterns in dynamic tasks such as walking.

1. Introduction

Musculoskeletal redundancy (Bernstein, 1967) in biomechanical models is often addressed through optimizations that identify a unique muscle activation pattern among many possible. One popular criterion is minimizing muscle stress (Crowninshield and Brand, 1981) which has been widely applied to predict muscle coordination in simulations (Anderson and Pandy, 2001; Thelen et al., 2003; Erdemir et al., 2007). However, measured muscle activity often varies significantly from these predictions (Buchanan and Shreeve, 1996; Herzog and Leonard, 1991; Thelen and Anderson, 2006; van der Krogt et al., 2012). We currently lack methods for analyzing high-dimensional musculoskeletal models that would allow us to quantify the degree to which muscle activity may feasibly vary for a given motor task.

The first step to understand the variability in muscle activity with respect to musculoskeletal redundancy is to identify absolute biomechanical constraints on muscle activity for a given task. In contrast to optimization, this approach seeks to find the full range of possible solution sets available to the nervous system (Kutch and Valero-Cuevas, 2011). In particular, identifying the explicit bounds on muscle activation can reveal whether predicted or measured muscle activity is due to biomechanical requirements necessary to perform the task, or because of allowable variability in how the task can be achieved. Identifying feasible bounds of muscle activity can also describe the degree to which muscle activity may deviate from optimal solutions.

This study was motivated by experimentally-observed inter- and intra-subject variability during reactive balance control (Horak and Nashner, 1986; Torres-Oviedo et al., 2006; Torres-Oviedo and Ting, 2007). For example in cats, when producing an extensor force vector (Fig. 1A, F_{EXT}), knee extensor *vastus medialis* (VM) was recruited consistently across animals, but hip and knee flexor *medial sartorius* (SARTm) was recruited at different levels across animals (Fig. 1B, F_{EXT}). Conversely, when producing a flexor force vector (Fig. 1A, F_{FLEX}), VM recruitment varied across animals but SARTm was recruited consistently in all animals (Fig. 1B, F_{FLEX}).

Here, we identified feasible ranges of muscle activation during static force production in a detailed model of the cat hindlimb

* Corresponding author at: Department of Biomedical Engineering, Georgia Institute of Technology and Emory University, 313 Ferst Drive, Atlanta, GA 30332-0535. Tel.: +1 404 894 5216.
E-mail addresses: lting@emory.edu, lena.ting@bme.gatech.edu (L.H. Ting).

0021-9290/$ - see front matter © 2013 Elsevier Ltd. All rights reserved.
http://dx.doi.org/10.1016/j.jbiomech.2013.01.020

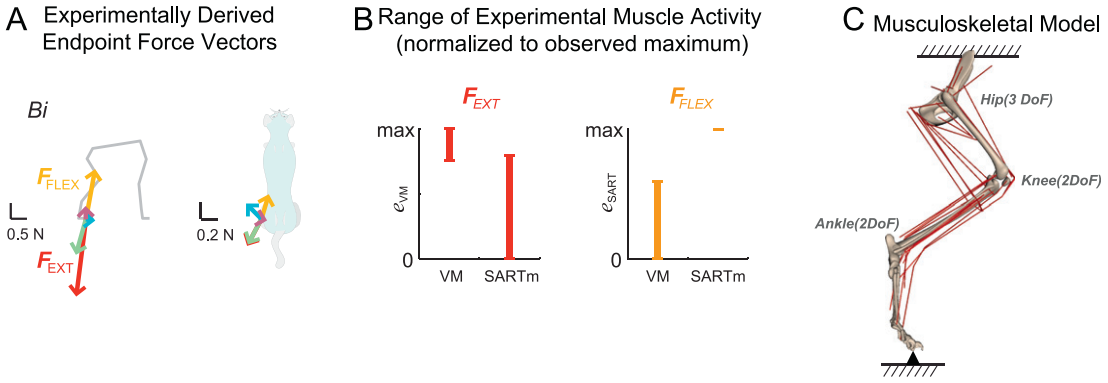

Fig. 1. (A) Experimentally-measured hindlimb endpoint force vectors in cat *Bi* from Torres-Oviedo et al. (2006). Extensor force vector (F_{EXT}, red) and flexor force vectors (F_{FLEX}, yellow) were essentially identical across cats. (B) Range of experimental muscle activity for producing F_{EXT} and F_{FLEX} across 3 cats. When producing F_{EXT}, VM was consistently activated in all animals, whereas the activation level of SARTm varied across animals. For F_{FLEX}, SARTm was activated consistently in all animals and VM was activated at varying levels across animals. (C) Musculoskeletal model of the cat hindlimb (Burkholder and Nichols, 2004) with seven rotational degrees of freedom (3 at the hip, 2 each at the knee and ankle) and 31 muscles. In this static model, the pelvis was fixed to the ground and the endpoint, defined at the MTP joint, was connected to the ground via gimbal joint where moments were constrained to be zero.

(Fig. 1C; Burkholder and Nichols, 2004; McKay and Ting, 2008). We identified the upper and lower bounds on muscle activity in each of 31 muscles during endpoint force production in different directions and magnitudes. Muscles with non-zero lower bounds were classified as "necessary", whereas muscles with zero lower bounds were classified as "optional". Muscles were further classified to have "submaximal upper bound" or "maximal upper bound". To examine the degree to which feasible muscle activation patterns could deviate from an optimal solution, we compared these bounds to muscle activation patterns predicted by minimizing muscle stress (Crowninshield and Brand, 1981), or scaling the pattern required for maximum force generation (Valero-Cuevas, 2000).

2. Methods

2.1. Musculoskeletal model

The static three-dimensional musculoskeletal model of the cat hindlimb (Burkholder and Nichols, 2004) included seven rotational degrees of freedom (Fig. 1C). 31 muscles (Table 1) produced net joint torque $\vec{\tau}$ (7×1), and a resulting endpoint wrench (force and moment vector) $\vec{F}_{End}$ (6×1) at the metatarsophalangeal (MTP) joint. The MTP was connected to the ground via a gimbal joint (Fig. 1C), representing the experimental condition of a freely standing cat where the foot never lost contact or slipped with respect to the ground (Jacobs and Macpherson, 1996). Endpoint moments were constrained to be zero, a conservative approximation of the small moments that can be supported by the contact area of cat's foot (McKay et al., 2007). The model defined the mapping from muscle activation vector $\vec{e}$ (31×1) to endpoint wrench $\vec{F}_{End}$:

$$\boldsymbol{RF}_{AFL}\vec{e}=\vec{\tau}=\boldsymbol{J}^{T}\vec{F}_{End}, \quad (1)$$

where $\boldsymbol{J}$ is a geometric Jacobian (6×7), $\boldsymbol{R}$ is a moment arm matrix (7×31) that maps muscle forces to joint torques, and $\boldsymbol{F}_{AFL}$ is a diagonal matrix (31×31) of scaling factors based on the active force–length property of muscle (Zajac, 1989). To approximate the operating region on the force–length relationship curve commonly observed in habitual postures, all muscles were set to 95% optimal fiber length (Burkholder and Lieber, 2001; Roy et al., 1997; Sacks and Roy, 1982). We found matrices $\boldsymbol{J}$ and $\boldsymbol{R}$ for each of 3 cats *Bi*, *Ni*, and *Ru* based on their average kinematic configuration measured during quiet standing (McKay et al., 2007) using Neuromechanic software (Bunderson et al., 2012).

2.2. Target endpoint forces

Five experimentally-derived force vectors in each cat measured during postural responses to translational support perturbation (Torres-Oviedo et al., 2006) were used as target endpoint force vector directions (Fig. 1A). These force vectors represented the active response of the cats following perturbation, measured as the change in the ground reaction force from the background level, averaged over the postural response period 150–200 ms following the perturbation (Jacobs and Macpherson, 1996), where only small angular deviations in joint angles ($\leq2^{\circ}$) are observed (Ting and Macpherson, 2004). To examine biomechanical constraints across force magnitudes, we scaled each force vector from 0 to the maximum feasible level that could be produced by the model, identified using linear programming. We found the muscle activation pattern $\vec{e}^{\,MAX}$ that maximized force magnitude:

$$\vec{e}^{\,MAX}\text{: Find } \vec{e} \text{ s.t. } \|(\boldsymbol{RF}_{AFL}\vec{e}).(\boldsymbol{J}^{T}\vec{F}_{Exp})\| \text{ is maximized, while } (\boldsymbol{RF}_{AFL}\vec{e})\times(\boldsymbol{J}^{T}\vec{F}_{Exp})=0, \quad (2)$$

where the cross product constraint in Eq. (2) ensured the preservation of force direction. Activation of each muscle was constrained between 0 and 1, and endpoint moments were constrained to be zero. The maximum feasible force in direction of the experimental force vector is given by:

$$\vec{F}_{EXP}^{MAX}=\boldsymbol{RF}_{AFL}\frac{\vec{e}^{\,MAX}}{\boldsymbol{J}^{T}\vec{F}_{Exp}}\vec{F}_{Exp}. \quad (3)$$

2.3. Lower and upper bounds on muscle activation

We used linear programming to identify the lower bound ($e_m^{\boldsymbol{LB}}$) and the upper bound ($e_m^{\boldsymbol{UB}}$) on the feasible activation level of each muscle as the magnitude (α) of each of the target endpoint force vectors was scaled from 0 to 1 (Eqs. (4) and (5)). Grid spacing $\Delta\alpha=0.1$ was used from $\alpha=0.0$ to 0.9, and grid spacing $\Delta\alpha=0.02$ from $\alpha=0.9$ to 1.0 because initial tests revealed rapid changes for higher values of α. For each muscle and each value of α, the lower and upper bound was identified as follows:

$$e_m^{\boldsymbol{LB}}\text{: Find } \vec{e} \text{ s.t. } |e_m| \text{ is minimized, while } \boldsymbol{RF}_{AFL}\vec{e}=\alpha\boldsymbol{J}^{T}\vec{F}_{Exp}^{MAX} \quad (4)$$

$$e_m^{\boldsymbol{UB}}\text{: Find s.t. } |e_m| \text{ is maximized, while } \boldsymbol{RF}_{AFL}\vec{e}=\alpha\boldsymbol{J}^{T}\vec{F}_{Exp}^{MAX} \quad (5)$$

Each muscle was classified as *necessary* or *optional* based on whether, and at what force magnitude the muscle became biomechanically required to generate

Table 1
Muscles included in the hindlimb model and abbreviations.

Name	Abbreviation	Name	Abbreviation
Adductor femoris	ADF	*Plantaris*	PLAN
Adductor longus	ADL	*Iliopsoas*	PSOAS
Biceps femoris anterior	BFA	*Peroneus tertius*	PT
Biceps femoris posterior	BFP	*Pyriformis*	PYR
Extensor digitorum longus	EDL	*Quadratus femoris*	QF
Flexor digitorum longus	FDL	*Rectus femoris*	RF
Flexor hallicus longus	FHL	*Sartorius*	SART
Gluteus maximus	GMAX	*Semimembranossus*	SM
Gluteus medius	GMED	*Soleus*	SOL
Gluteus minimus	GMIN	*Semitendinosus*	ST
Gracilis	GRAC	*Tibialis anterior*	TA
Lateral gastrocnemius	LG	*Tibialis posterior*	TP
Medial gastrocnemius	MG	*Vastus intermedius*	VI
Peroneus brevis	PB	*Vastus lateralis*	VL
Pectineus	PEC	*Vastus medialis*	VM
Peroneus longus	PL		